CHAPTER IV

ab initio STUDIES OF IRON AND SILVER

4.1 INTRODUCTION

Applications of simulations enter into all domains of science and technology. Nanotechnology and electronics are the most popular new technologies. Understanding the detailed electronic structure of materials has been a challenging problem in electronics.

For understanding the electronic properties of materials three approaches have been developed during the past hundred years. "Continuum theory" considers only macroscopic quantities that are interrelated to experimental data. No assumptions were made about the structure of matter when the equations were formulated. The "Classical electron theory" postulated that free electrons in metals drift as a response to an external force and interact with certain lattice atoms. Paul Drude was the principal proponent of this approach and his equations are still widely utilized today. The "Quantum theory" is able to explain important experimental observations which could not be readily interpreted by classical means. The features of this theory, such as, Fermi energy, density of states, Fermi distribution function, band structure, Brillouin zones, effective mass of electrons, quantization of energy levels etc., are important properties for understanding the materials. Furthermore, measurements of electric and electronic properties of crystals require a specified laboratory, as well as excellent quality materials, which generally is expensive.

The use of quantum mechanical calculations to predict accurately the structure and properties of crystals is going to have significant implications for the studies of materials. Recently self-consistent *ab initio* calculations within density functional theory using super-cell models are successful in tackling the problem.

ab initio calculations have gained recognition, because they have shown to be important when predicting the properties of new materials. Currently this

technique is too demanding computationally to apply to large structures. It is clear, however that with the continuing increase in the available computing power and rapid development of new theoretical approaches, the range of investigations is going to grow dramatically.

The understanding of the behavior of electrons in solids is one of the keys to understand materials. The electron theory of solids is capable of explaining optical, magnetic, thermal and electronic properties of materials. The electron theory provides important fundamental ideas for a technology which is often considered to be the basis for modern electronic devices. The main tools used in *ab initio* solid state computer experiments are density functional theory (DFT) and periodic boundary conditions. The DFT methods are used to calculate structural, optical, electronic and vibrational properties of low dimensional system. Density functional theory is an alternative for predicting the properties with good agreement. DFT has gained considerable momentum over the past 40 years since its inception, and even more so in the past 10 years: workstation power has risen and at the same time the size of objects accessible to experiment has shrunk, such that now there is a growing overlap between what can be simulated and what can be characterized in the lab. Thus DFT is not the final theory of atomic and solid-state systems, but its failures and limitations are beginning to be well mapped out. Cambridge serial total energy package is a state of the art quantum mechanics based program designed specifically for solid-state materials science. DFT is in practical terms the only approach that allows one to treat electron gas in solids for any realistically interesting number of atoms in the unit cell. The tools that are specific to CASTEP include norm-conserving pseudo-potential, plane wave basis set, the use of k point sampling techniques, BFGS scheme for geometry optimization etc.

CASTEP employs the density functional theory plane wave pseudo-potential method which allows us to perform first-principles quantum mechanics calculations that explore the properties of crystals and surfaces in materials, such as, metals, semiconductors, ceramics, minerals and zeolites. The major advantages of the plane wave based approach are, the ease of computing forces and stresses, good

convergence control with respect to all computational parameters employed; favorable scaling with the number of atoms in the system and the ability to make cheaper calculations by neglecting core electrons. Typical applications involve studies of surface chemistry, structural properties, band structure, density of states and other properties. It can also be used to study the spatial distribution of the charge density and wave functions of a system. Thus this program provides a robust and efficient implementation of DFT which is based on the following concepts:

Pseudo-potential description of the electron-ion interaction

- Super cell approach with periodic boundary conditions
- Plane wave basis set
- Extensive use of Fast Fourier Transform (FFT) for evaluation of the Hamiltonian terms
- Iterative schemes for the self-consistent electronic minimization
- Implementation of the most popular DFT expressions for the exchange- correlation functional, including the screened and exact exchange schemes.

CASTEP is based on a super cell method, wherein all studies must be performed on a periodic system, even when the periodicity is super cell. Thus, for example, a crystal surface must be represented by a finite-length slab. Similarly to study molecules, it is necessary to assume that they are in a box and treat them as periodic systems. There is no limitation on the shape of the super cell. The main advantage of imposing periodic boundary conditions relates to Bloch's theorem, which states that in a periodic system each electronic wave function can be written as a product of a cell-periodic part and a wave-like part.

The structural and electronic properties of one dimensional material are calculated from first principles, using the density functional theory. Density Functional Theory is presently the most widely used framework for the simulation of the electronic structure of materials and molecules. Its scope is very large and in principle can cover the prediction of properties of the ground state of any system of

electrons. Relativistic extensions exist and the coupling to classical electromagnetic fields is becoming commonplace. DFT is a delicate balance between precision and numerical tractability.

There are a number of approximations which are usually made in order to render the computations accessible to present-day computers, and a few standard extensions (more precision for a higher computational cost) are mentioned. In brief the final limitation is computer power. The more operations per second can be executed, the larger the systems can be calculated and the greater the precision and the appetite for new systems is infinite.

Recent band structure calculations based on *ab initio* methods, baring new tools to calculate the full dispersion of the band and as a consequence of the effective masses. An extensive experimental investigation has carried out on Fe and Ag metals, but a detailed theoretical knowledge is required to understand the electronic structure of Fe and Ag for its suitability for applications. However, even for most of the well-known photovoltaic materials, an important dispersion between experimental to theoretical data is not found in any published literature. Although simple and formal perturbation theory, the important parameters in the model have not been known with efficient accuracy to render the validity of the theoretical results. The reason for this is depending on different approaches to the band structure calculations, mainly in the empirical methods, where the main objective is to reproduce energy values at high geometry points where the correct dispersion of the bands is not well predicted.

4.2 SURVEY OF LITERATURE for *ab initio* STUDIES

4.2.1 Survey of literature for *ab initio* studies of Fe

Riikonen et al., (2010) have studied various α-iron (ferrite) facets at different carbon concentrations using *ab initio* methods. In the case of α-iron, the morphology of (110), (100), and (111) facets is quite different. This can result in very different diffusion barriers, carbon-carbon bond formation energetics and

kinetics. For a better understanding of the experiments it is important to perform *ab initio* simulations and correlate computational results to the phenomena observed in the in situ studies.

Kevin M. Rosso et al., (2003) have discussed the transport of conduction electrons through basal planes of the hematite lattice modeled as a valence alternation of iron cations using *ab initio* molecular orbital calculations and electron transfer theory. A cluster approach was successfully implemented to compute electron-transfer rate-controlling quantities such as reorganization energy and electronic coupling matrix element. Localization of a conduction electron at an iron lattice site is accompanied by large iron–oxygen bond length increase that gives rise to a large internal component of the reorganization energy ~1.03 eV. The internal reorganization energy calculated directly is shown to differ from Nelsen's four-point method due to the short-range covalent bridge interaction between the Fe–Fe electron transfer pair in the hematite structure. The external reorganization energy arising from modification of the lattice polarization surrounding the localization site is predicted to contribute significantly to the total reorganization energy. Therefore the localized electron treatment is appropriate to describe electron transport in this system. Thus **Rosso et al.,** applied *ab initio* cluster model strategy to understand Fe (II/III) electron hopping in hematite basal planes. Based on bond length changes in the clusters after the addition of an extra electron, the position of the electron is predicted to be strongly localized. The extra electron causes large increase in the Fe–O bond lengths of the Fe octahedron in which it resides, leading to large internal reorganization energy.

Postnikov et al., (2003) have calculated from first-principles the electronic structure, relaxation and magnetic moments of small Fe particles, by applying the numerical local orbitals method in combination with norm-conserving pseudo potentials. The accuracy of the method in describing elastic properties and magnetic phase diagrams is tested by comparing benchmark results for different phases of crystalline iron to those obtained by an all electron method. Their calculations for the bipyramidal Fe_5 cluster confirmed the previous plane-wave results that predicted

a non-collinear magnetic structure. For larger bcc-related (Fe_{35}, Fe_{59}) and FCC-related (Fe_{38}, Fe_{43}, Fe_{55}, Fe_{62}) particles, a larger inward relaxation of outer shells has been found in all cases, accompanied by an increase of local magnetic moments on the surface to beyond 3μB.

Taylor et al., (2015) have revealed through *ab initio* ET calculations that OS (Outer-sphere) ET (electron transfer) was strongly kinetically inhibited in all cases modeled. OS ET as a concerted proton-coupled ET reaction (ferrimagnetic spin configuration) is thermodynamically favorable (-35 kJ/mol), but kinetically inhibited by concurrent proton-transfer (10^{-19} s^{-1}). A more fundamental understanding of mechanisms involved in the abiotic reduction of U (VI) by Fe (II) has been gained by combining experiments and *ab initio* modeling. With the help of *ab initio* calculations they revealed the nature of thermodynamic and kinetic barriers that must be overcome at the molecular scale in order for reduction to proceed in a homogeneous system, such as dehydration of solvated complexes and Fe^{2+} hydrolysis. In turn, reduction of U (VI) by Fe (II) in a homogeneous system is predicted to be kinetically inhibited. These atomistic details are difficult to observe using geochemical models or experiments, and have helped reinforce deductions from experiments. Their results not only show the reduction of soluble U(VI) by soluble Fe(II) to be thermodynamically and kinetically limited under experimental conditions, but also and most importantly, shed light on the feasibility of uranyl reduction in a homogeneous system under different chemical conditions (e.g., in the presence of naturally occurring reductants such as sulfide and hydroquinone).

Artem et al., (2005) explained about *ab initio* simulations which becomes a powerful tool for studies of matter, especially at extreme conditions where experimental information is limited. Since this tool is relatively new in planetary sciences, there are many open problems awaiting the application of such simulations. Also they have analyzed Density functional theory (DFT) which is the most popular (and usually the most accurate) basis for *ab initio* simulations. However, it has serious problems in describing Vander Waals bonding and seriously underestimates band gaps in solids. The solution of the band gap problem is

essential for the studies of metallization under pressure. This problem is especially acute for Mott insulators, many of which (e.g., FeO) are represented as metals in standard DFT calculations. Mott insulators play a very special role in the Earth's mantle and core-mantle boundary, therefore further progress of computational methodology is needed for a wider application of the first-principles simulation techniques in Earth and planetary sciences.

Joohee Lee and Seungwu Han (2013) investigated the native point defects in Fe_2O_3 using *ab initio* methods based on the GGA + U formalism. They considered vacancies and interstitials of Fe and O atoms, determining the formation energies and charge transition levels of each defect type in the isolated limit. It was found that $Fe_{(I)}$ and $V_{(Fe)}$ form shallow donor and acceptor levels, respectively, and therefore these are the defect types that may introduce carriers under ambient conditions. They determined the oxygen deficiency under high-temperature equilibrium conditions and an excellent agreement with the previous experiment was found. In the quenched condition, it is found that the Fermi levels are pinned at ~0.5 eV below the conduction band minimum, which may limit the performance of Fe_2O_3 as photo anodes of solar water-splitting cells. They found that V_O is neutral under ambient conditions and $Fe_{(I)}$ is responsible for electron carriers. Having established the fundamental electronic character of point defects, it is believed that the present results will provide useful information for optimizing the material properties of Fe_2O_3.

Manh-Thuong Nguyen et al., (2014) in their work, used the density functional theory (DFT) calculations at the PBE+U level of theory and investigated the properties of hematite surfaces induced by O and Fe vacancies, Al substitutional impurities, and Fe and Al atoms. They first determined the formation energy of such defective sites as a function of μ_o. The defect-induced geometry relaxation was then examined. The electronic properties and reactivity with oxygen of some defects were finally addressed. Under oxygen rich conditions, all defects are metastable with respect to the ideal surface. Under oxygen-poor conditions, O vacancies and Fe atoms become stable. Under ambient conditions, all defects are metastable; in the

bulk, O vacancies form more easily than Fe vacancies, whereas at the surface the opposite is true. All defects, that is, O and Fe vacancies, Fe and Al atoms, and Al substituents, induce important modifications to the geometry of the surface in their vicinity. Dissociative adsorption of molecular oxygen is likely to be exothermic on surfaces with Fe/Al atoms or O vacancies.

Shih-Yun Chen et al., (2009) have demonstrated that the O K edges of hematite and goethite can be computed utilizing *ab initio* method. Using *ab initio* calculations they showed how electron energy loss spectroscopy (EELS) can be used in order to characterize phases of iron oxide/hydroxide nanomaterials. In particular, they showed that dehydration of iron hydroxide such as goethite can easily appear under the electron beam but might be followed by monitoring the O K peak. Indeed, both LSDA and LSDA+U calculations confirm that the intensity of the pre-peak of the O K should increase while H atoms are removed, either under the heating or knock-on effect from the electron beam. The influence of the hydroxyl bonding in the prepeak shape of the O K edges of iron oxides is thus discussed. These results suggest that high-energy resolved EELS on O K edges can probe the local average connectivity of oxygen with iron and can be useful to distinguish between iron oxide and iron hydroxide on nanometer scale.

4.2.2 Survey of literature for *ab initio* studies of Ag:

Dmitri S. Kilin et al., (2008) indicated that the *ab initio* electronic structure calculations for citric acid are much more likely to bind to the silver (111) surface than to the (100) surface at room temperature. The preferential binding is stipulated by the following factors: (i) coincidence of the symmetries of the ligand and the surface; (ii) matching in the size of the ligand and the surface lattice constant; and (iii) activation of the ligand electronic structure by hydrogen atom migration. The binding of citric acid to the silver surfaces proceeds through the two methylene-carboxyl groups. Good symmetry and geometry agreement between the acid and the (111) surface produces four ligand surface bonds. Although the carboxyl group does not directly bind to (111) either, it activates all for oxygen atoms of the methylene-

carboxyl groups by accepting a hydrogen atom from these groups. The quadric difference in the energy of binding of citric acid to the silver (111) and (100) surfaces can be decomposed into the factor of two enhancements due to the doubling of the number of the ligand-surface bonds and an additional factor of two achieved by activation of the ligand electronic structure due to the hydrogen atom migration. The reported theoretical study fully supports and explains the experimental observation that citric acid passivates the (111) surfaces of silver nanocrystals and permits growth of the (100) surfaces, providing control over the nanoparticle shape.

Monica Garcia et al., (2015) have combined first-principles atomistic thermodynamics with a Wulff–Kaichew construction to determine the equilibrium shape of Ag particles supported on α-Al_2O_3 (0001) under gas-phase conditions representative for ethylene epoxidation. Overall, this is fully consistent with the common description of hemispherical Ag microcrystals on this support, but at variance with the cubic Ag nanoparticles.

Gebhu F Ndlovu et al., (2012) determined that the *ab initio* calculations confirm the lowest potential energy between Ag and the graphene structure to be at the exact site determined from STM imaging. In order to confirm the preference of Ag sitting on top of C atoms rather than at the bridge or in the hollow sites of the C hexagon, an *ab initio* study was necessary. The effect of Ag on the electronic structure of graphene was further investigated by them. They also predicted direct band gap which can be seen from the band structure. Also they employed first-principles of density functional theory in order to verify experimental observations.

Xo chitl Lopez-Lozano et al., (2014) presented *ab initio* time dependent density-functional theory calculations of pentagonal Au and Ag rods with up to 145 atoms, corresponding to a length of 7 nm. The transition is geometry related and entirely different from the size-dependent appearance of the SPR in spherical particles. Comparison with thicker rods with up to 263 atoms and with linear Ag and Au chains shows that by changing the aspect ratio and absolute size, the resonance energy can be tuned in and out of the region where the coupling with the inter-band

transitions leads to strong damping of the SPR, thus changing the character of the optical response decisively.

Molina et al., (2014) performed *ab initio* density functional simulations to study the adsorption of propene on partially oxidized silver surfaces and its interaction with surface oxygen. Two different adsorption conformations for propene are studied, with the molecule either intact or forming an Ag–C_3H_6–O oxymetallacycle (OMC) intermediate. Then, pathways for propene oxide, acrolein and propanone formation have been studied in detail, providing insight into the selectivity of the surfaces. It is found that the formation of acrolein must necessarily take place from OMC intermediates, requiring at least two neighbouring reactive surface oxygen anions. This suggests a strong relationship between the concentration of surface oxygen and the selectivity of these surfaces.

Amanda et al., (2012) have used a time-domain *ab initio* approach, and investigated the phonon-induced relaxation dynamics of plasmon excitations in a silver nanoparticle. The relaxation occurs on a picosecond time scale, in agreement with the experimental data. It is established that plasmon excitations are weakly coupled to phonons, in particular, because they are spatially delocalized away from the nanoparticle core. Only low-frequency acoustic modes are able to facilitate the energy decay because only these modes can modulate plasmon wave functions and energies. The effects of high-frequency vibrations on plasmon states tend to average out, when integrated over the delocalized plasmon wave functions. The higher energy plasmon excitations are both more delocalized and tend to exhibit weaker coupling to phonons. This explains the different decay time scales for low and high-energy excitations observed in experiments. The elastic phonon-induced pure-dephasing of plasmon excitations is two orders of magnitude faster than the inelastic plasmon-phonon scattering and involves higher frequency phonons. The charge−phonon interactions in semiconductor quantum dots and nanoscale carbon materials are stronger than the plasmon−phonon interactions. As a result, both elastic and inelastic charge−phonon scattering processes are faster than their corresponding plasmon−phonon scattering counterparts. Whereas elastic phonon-

induced pure-dephasing creates a notable contribution to the line width of plasmon resonances, the contribution of the phonon-induced energy decay to the line width is negligible. At the same time, the energy of plasmon excitations is ultimately deposited into the phonons. The simulations used in the study show that the transfer of energy from plasmon excitations into acoustic phonons of metallic nanoparticles proceeds within a few picoseconds.

Luque et al., (2012) have investigated *ab initio* calculations for the geometry, energetic, and electronic properties of L-cysteine adsorption on Ag (111), not only qualitatively but also quantitatively using density functional theory. An exhaustive analysis has been performed using DFT calculations. The adsorption energy increases with coverage. At low coverage, a flat configuration exists where not only the sulfur atom but also the carboxyl group strongly interacts with the surface. Zwitterionic species have been found to be more favorable at higher coverages. It is noticeable that silver atoms in the second and third layer below the surface show changes in their electronic distribution. The formation of bonds between the adsorbate and the metal involves the simultaneous participation of different orbitals given a complicated hybridization feature. Bonds with σ and π character are formed. Also the electronic states of the α-carbon atom participating in the bond with the sulfur atom are affected.

4.3 COMPUTATIONAL DETAILS

4.3.1 Calculation Method

Calculations of the band structure, density of states, optical spectra and dielectric functions of the Fe and Ag crystals have been performed using the CASTEP code and a DFT plane wave pseudo-potential program within the frame work of local density approximation and generalized gradient approximation for the exchange correlation effects. The ultra soft model pseudo-potentials are used. This pseudo-potential requires a quite low energy cut off and guarantees good transferability, that is the same potential correctly reproduces the valence electron scattering by the ion core in different chemical environments. Calculations are

performed using the plane wave basis set with the kinetic energy cut off for plane wave 300 eV, which corresponds to the energy convergence criterion of self-consistency of $0.2x10^{-5}$ eV/atom. The optimization of crystal structure has been performed with the characteristic tolerances for total energy $0.2x10^{-4}$ eV /atom, and root mean square stress tensor 0.1GPa, before the calculations of band structure. Each energy state of the crystals is calculated at 10 k-points of Brillouin zone.

4.3.2 Structural Optimization

The crystal structure and locations of the particular atoms of Fe and Ag have been determined from X-ray diffraction data. The cut off energy of 270 eV was assumed in the plane wave basis set. Optimization (relaxation) of the atomic positions and crystal cell parameters was performed before the main calculations of electronic characteristics: total electronic energy E, band energy dispersion, density of electronic states and dielectric functions.

4.3.3 Brillouin Zone Sampling

Electronic states are allowed only at a set of k-points determined by the boundary conditions that apply to the bulk solid. The infinite number of electrons in the periodic solid is accounted for an infinite number of k-points. The Bloch theorem changes the problem of calculating an infinite number of electronic wave functions to one of calculating a finite number of wave functions at an infinite number of k-points. The occupied states at each k-point that are very close together will be almost identical. This suggests that the DFT expressions that contain a sum over k-points (or, equivalently, an integral over the Brillouin zone) can be efficiently evaluated using a numerical scheme that performs summation over a small number of special points in the Brillouin zone. In addition, symmetry considerations suggest that only k-points within the irreducible segment of the Brillouin zone should be taken into account. An accurate approximation of the electronic potential and the total energy of an insulator can be obtained by calculating electronic states at a very small number of k-points. The calculations for metallic systems require a more dense set of k-points to determine the Fermi level accurately.

4.3.4 Self-Consistent Electronic Minimization

CASTEP offers a choice of methods for electronic relaxation. The default method is the most efficient and is based on density mixing. In this scheme the sum of electronic eigen values is minimized in the fixed potential instead of the self-consistent minimization of the total energy. The new charge density at the end of the minimization is mixed with the initial density and the process is repeated until convergence is reached. A number of options are supported for this scheme: linear mixing, Kerker mixing, Broyden mixing and Pualy mixing, in order of increasing robustness. The conjugate-gradient based approach is used to minimize the sum of Eigen values. A slightly more elaborate scheme that involves separate mixing of spin density has been developed for spin-polarized calculations. CASTEP also supports a more traditional scheme for electronic relaxation, involving minimization of the total energy. The electronic wave functions are expanded using a plane-wave basis set and the expansion coefficients are varied so as to minimize the total energy. This minimization is performed using an all-bands method that allows simultaneous update of all wave functions. The scheme uses a preconditioned conjugate gradients technique. The main advantage of the density of mixing method is its robustness for metallic systems, especially for metallic surfaces. A traditional total energy minimization scheme might become unstable in a metallic system with the cell elongated in one dimension and this is the typical set-up for the super cell calculations on surfaces. The density mixing scheme converges equally well for insulating and metallic cases and offers at least a factor of three speed-up moderately sized insulator systems.

4.3.5 Density of States and Partial Density of States

The density of states for a given band n, $N_n(E)$ is defined as $N_n(E) = \int \frac{dk}{4\pi^3} \delta(E - E_n(k))$, where En(k) describes the dispersion of the given band and the integral is determined over the Brillouin zone. An alternative representation of the density of states is based on the fact that $N_n(E)dE$ is proportional to the number of allowed wave vectors in the n^{th} band in the energy range from E to E+dE. The total density of states N(E), is obtained by summation over all bands. The

integral of N(E) from minus infinity to the Fermi level gives the total number of electrons in the unit cell. In a spin-polarized system one can introduce separate DOS for electrons with spin up and those with spin down. Their sum produces the total DOS and their difference is referred to as a spin density of states. The DOS is a useful mathematical concept allowing integration with respect to electron energy to be used instead of the integration over the Brillouin zone. In addition, the DOS is often used for quick visual analysis of the electronic structure.

Characteristics such as the width of the valence band, the energy gap in insulators and the number and intensity of the main features are helpful in qualitatively interpreting experimental spectroscopic data. DOS analysis can help to understand the changes in electronic structure caused by, for example, external pressure. There exist a variety of numerical techniques for evaluating the DOS. The simplest one is based on the Gaussian smearing of the energy levels of each band, followed by a histogram sampling. This method does not reproduce sharp features of the DOS, such as van-Hove singularities but it produces a satisfactory general shape of the DOS even with a small number of k-points used.

4.4 RESULTS AND DISCUSSION

4.4.1 Theoretical Study of Iron (Fe)

4.4.1.1 *ab initio* Studies of Structural Properties of Fe

The Fe structure was constructed using the software Materials Studio by fixing the atoms in a cube to form BCC structure. The constructed structures are optimized using the CASTEP module and given in Figure 4.1. The structure of Fe crystal at room temperature is found to be body centered cubic structure (BCC) with the unit cell dimensions 2.866 Å. The self consistent method of convergence of the structure is used to optimize the lattice parameters; the x-ray diffraction is simulated. The XRD spectra of the unit cells of Fe is simulated and given in Figure 4.2. X ray diffraction results of Fe reveals that they are crystalline nature with the prominent peak positions and the dominant structure of Fe is identified. The positions of the Fe

atoms are not defined experimentally and they are taken with different possible conditions, such that the results (XRD, band structure) are matched with the experimental values. Peak positions were analyzed from XRD spectrum and the positions of the miller indices in the x-ray diffraction spectrum of Fe unit cell are given in Table 4.1.

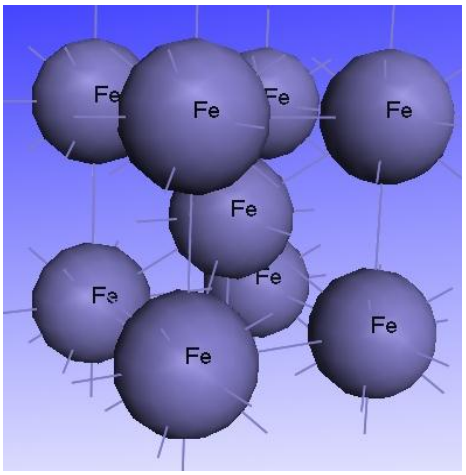

Figure 4.1 Structure of Fe (Body Centered Cubic Structure)

X-ray diffraction of the Fe nanoparticles prepared by precipitation method reveals that they are polycrystalline in nature with the prominent peak 110 of Fe. It exhibits BCC structure. The results are very close to the JCPDS data (870721) with lattice parameter 2.866 Å (a) and space group 229. The optimized BCC lattice parameter is 2.866 Å which is very close to the experimental value 2.8541 Å.

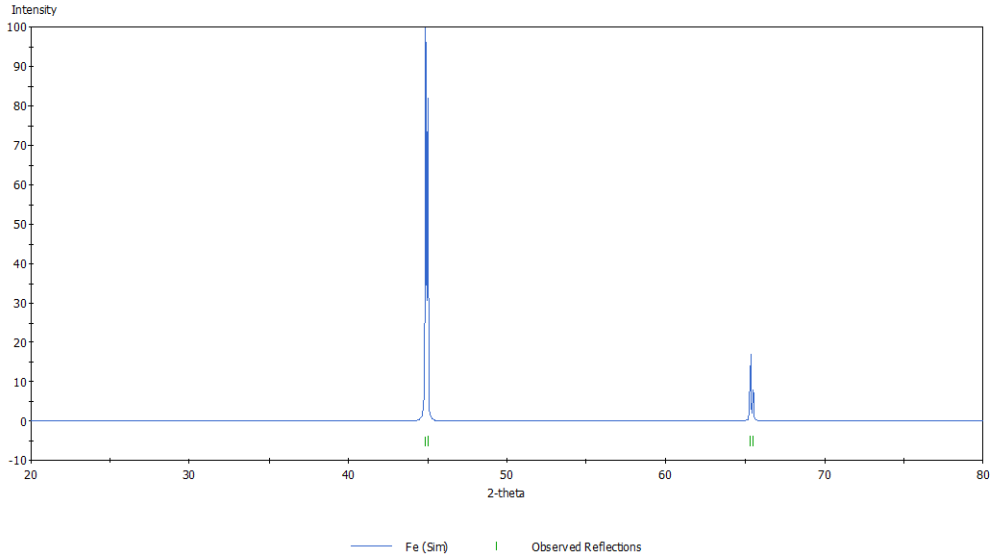

Figure 4.2 Simulated XRD pattern of FeBody Centered structure

Table 4.1 Miller indices of Fe structure

h	k	l	2Θ (SIMULATED)	INTENSITY (%)
1	1	0	44.88	100
1	1	0	45.00	82
2	0	0	65.35	17
2	0	0	65.50	8

The convergence of the structure is completed with the condition that LDA energy cut off 300 eV. The self consistent field convergence and self consistent field energy of the Fe structure have been obtained and shown in Figures 4.3 and 4.4 respectively.

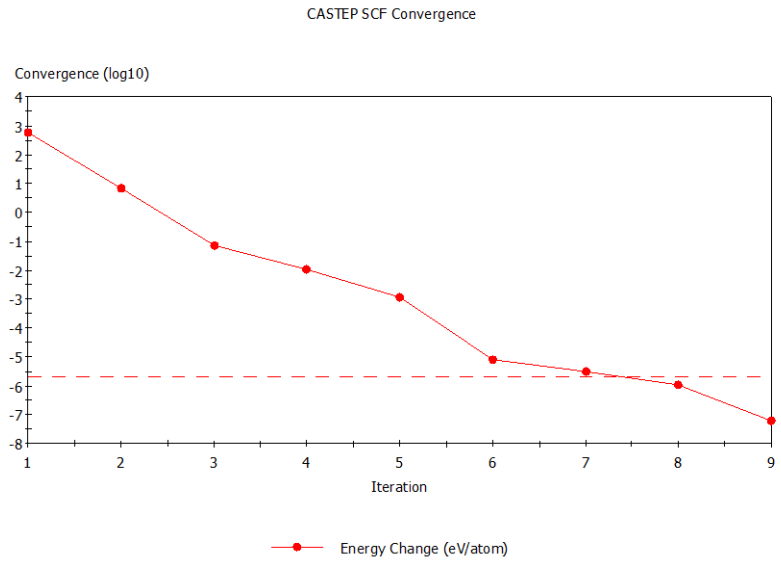

Figure 4.3 SCF convergence of Fe

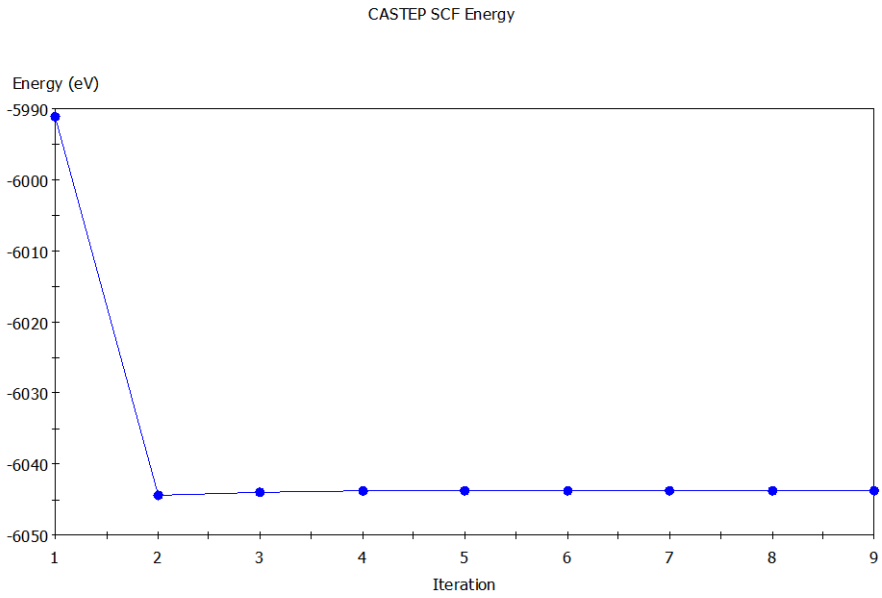

Figure 4.4 SCF energy of Fe

From the self-consistent method of convergence results, the lattice parameters are optimized and they are found to be very similar to the experimental results with slight deviation of 0.05 % to 0.06 % for Fe.

4.4.1.2 *ab initio* STUDIES OF ELECTRONIC PROPERTIES OF Fe

The calculations of electronic characteristics; total electronic energy E, band energy dispersion E (k) and density of states of Fe structure were simulated using the CASTEP code. Figures 4.5 and 4.6 illustrate the band structure and density of states of Fe respectively.

The total energy per atom convergence tolerance, smearing width and Fermi energy convergence tolerance are taken as $1x10^{-6}$ eV, 2×10^{-7} eV, 0.1 eV and 2×10^{-8} eV respectively. The band structure and density of states of Fe are calculated using LDA and are shown below,

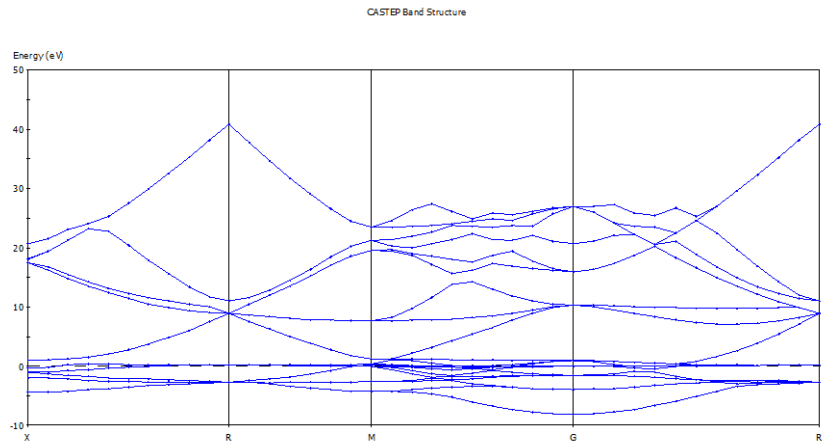

Figure 4.5 Band Structure of Fe

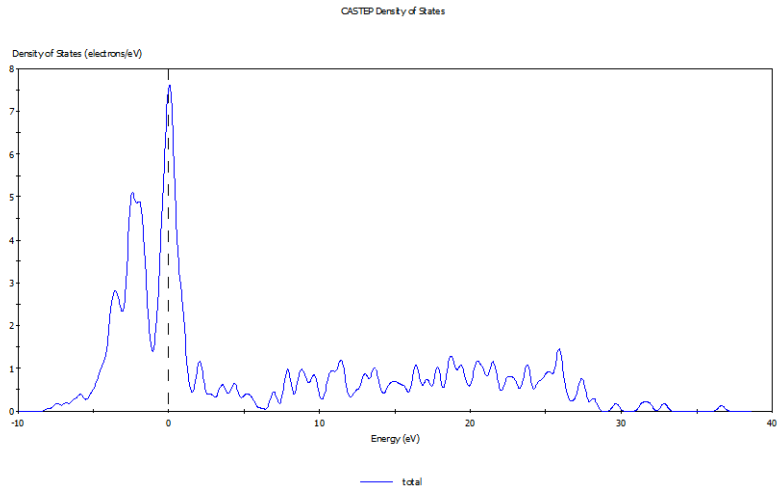

Figure 4.6 Density of states of Fe (LDA)

The band gap energy of Fe shows that there is a merging of valence band and conduction band. The density of states is dominated by a large peak near the Fermi

level which is responsible for the magnetic property of Fe (**Zhong et al., (1993)** and (**Nolting et al., (1995))**. The density of states of Fe was analyzed; it is observed that it is very much useful to predict the bond formation between Fe and other atoms, the electron life time in the bond formation, etc. (**Alaska subedi et al., (2008)**).

4.4.1.3 *ab initio* Studies of Optical Properties of Fe

Absorption, reflectivity, refractive index and extinction coefficients have been measured for Fe (BCC). The simulated absorption, reflectivity, refractive index and extinction coefficient studies of iron (Fe) are given in Figures 4.7, 4.8 and 4.9 respectively. Also the optical response functions for the Fe are calculated with the LDA and compared to the experimental data.

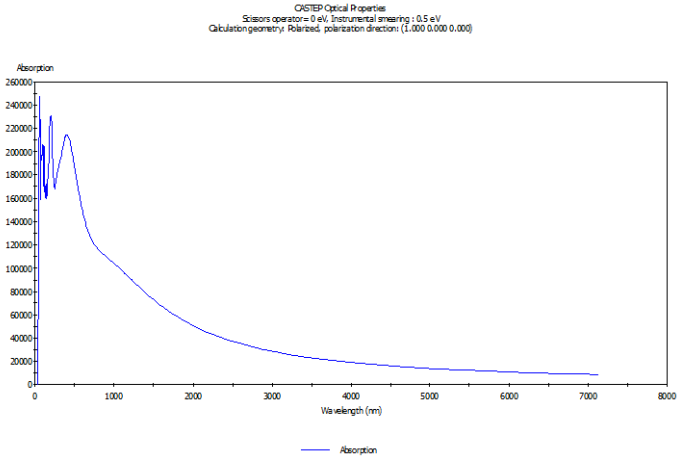

Figure 4.7Absorption spectrum of Fe (LDA)

It has been observed that the maximum absorption is observed at 3 eV which is very close to the experimental value of the earlier researchers.

The absorption study of the material is very important. Iron particles should have sufficient energy to penetrate into the cell walls of the bacteria or the biological cell structure of the animal or human.

The absorption energy of Fe is found as 3 eV which is sufficient to penetrate into the biological cells and react with enzymes and DNA structure.

More the absorption energy more will be the permeability of the nano material into the biological cells.

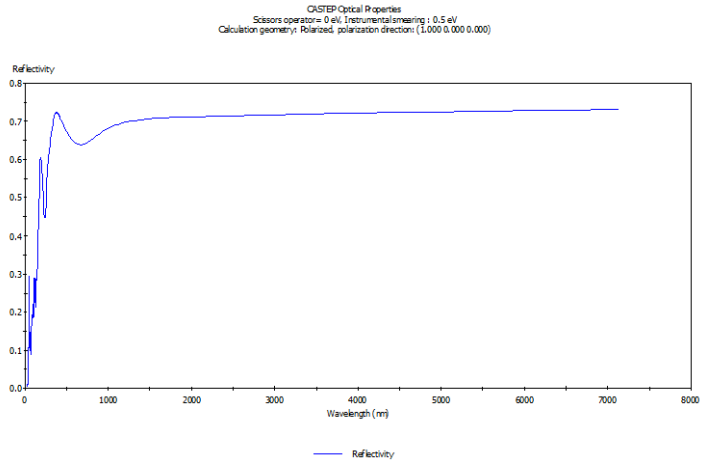

Figure 4.8 Reflectivity of Fe (LDA)

The reflectivity with wavelength was simulated using LDA as shown in Figure 4.8. In order to verify the counterpart of absorption and transmittance, the reflectivity of Fe has been studied. It has been observed that the reflectivity is maximum at 480nm.

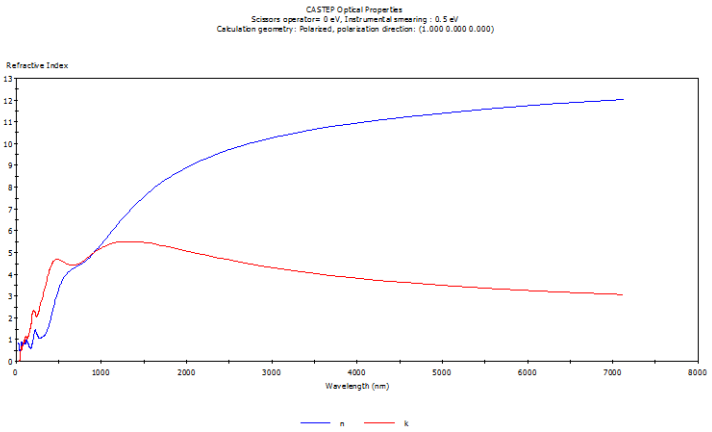

Figure4.9 Refractive index and Extinction coefficient of Fe (LDA)

The refractive index of a crystal is closely related to the electronic polarizability of ions and the local field inside the crystal. The refractive indices (n) and extinction coefficient (k) are fluctuating from 0 to 600 nm but increases gradually and becomes constant between 1500nm and 7000nm.

4.4.1.4 *ab initio* Studies of Dielectric Properties of Fe

The calculations of dielectric function, conductivity and loss function of Fe structure are simulated using the CASTEP code. Figures 4.10, 4.11 and 4.12 illustrate the dielectric function, conductivity and loss function of Fe respectively.

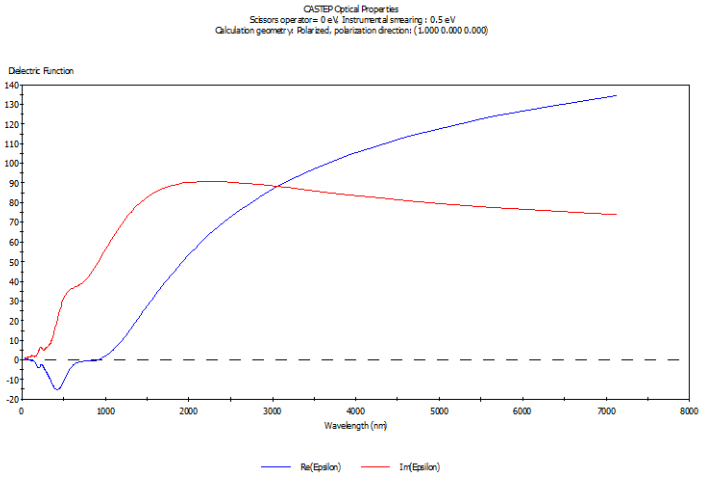

Figure 4.10 Dielectric Function of Fe (LDA)

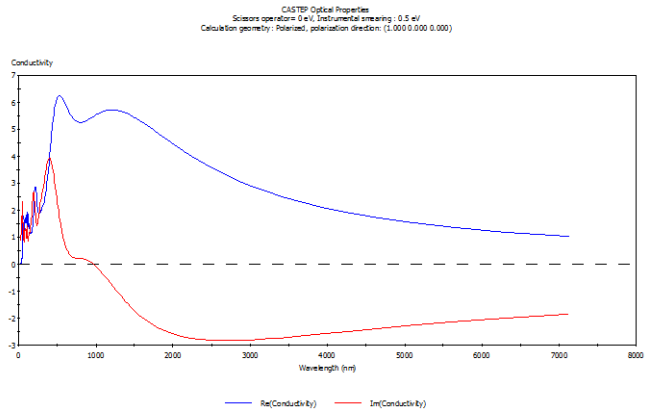

Figure 4.11Conductivity of Fe (LDA)

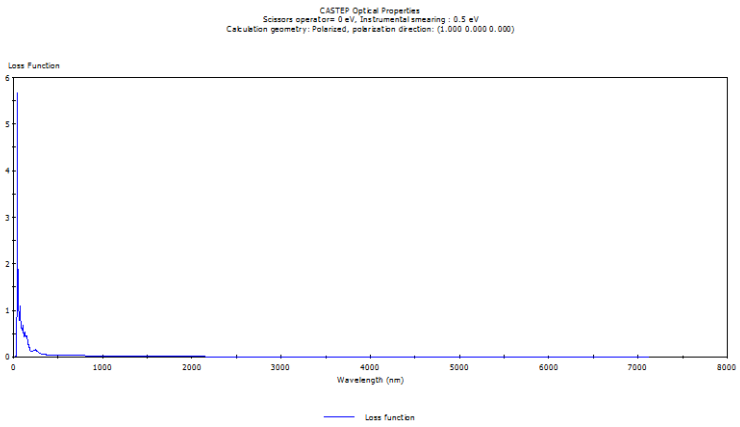

Figure 4.12 Loss Function of Fe (LDA)

The dielectric behavior of the material is necessary to know the interaction of the material with the medium or environment in which the material is present. Interestingly, the wavelength of 480 nm at which the real part of dielectric constant goes below zero as shown in Figure 4.10 is the wavelength at which the reflectivity is maximum as observed in Figure 4.8. The energy loss spectrum is related to the energy loss of fast electron traversing in the material, and is observed to be large at the lower wavelength region around 250 nm.

In the present study the nanoparticles of Iron are subjected to have interaction with the blood medium, bacteria and enzymes. An attempt is made to study the dielectric behavior of iron nanoparticles in blood and enzymes medium and find factors causing the biological changes in the cell structure.

4.4.2 Theoretical Study of Silver (Ag)

4.4.2.1 *ab initio* Studies of Structural Properties of Ag

The Ag structure was constructed using the software materials studio by fixing the atoms in a cube to form FCC structure. The constructed structures are optimized using the CASTEP module and given in Figure 4.13. The structure of Ag crystal at room temperature is found to be Face centered cubic structure (FCC) with the unit cell dimensions 4.085 Å. The self consistent method of convergence of the structure is used to optimize the lattice parameters; the x-ray diffraction is simulated

these XRD results are similar to that of the experimental XRD with the slight deviation of 0.05 % to 0.06 %.The XRD spectra of the unit cell of Ag was simulated and given in Figure 4.14. X ray diffraction results of Ag reveals that they are of crystalline nature with prominent peak positions and the dominant structure of Ag is identified. The positions of Ag atoms are not defined experimentally and they are taken with different possible conditions, such that the results (XRD, band structure) are matched with the experimental values. Peak positions were analyzed from XRD spectrum and the positions of the miller indices in the x-ray diffraction spectrum of Fe unit cell are given in Table 4.2.

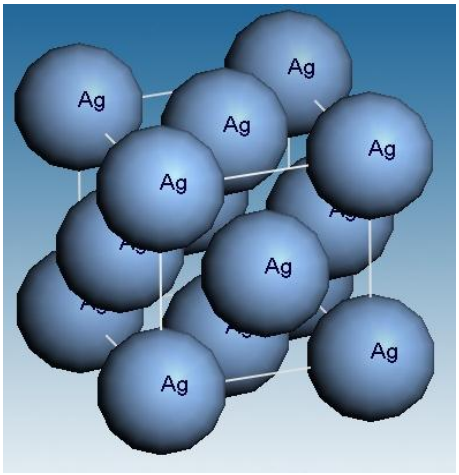

Figure 4.13 Structure of Ag (Face Centered Cubic Structure)

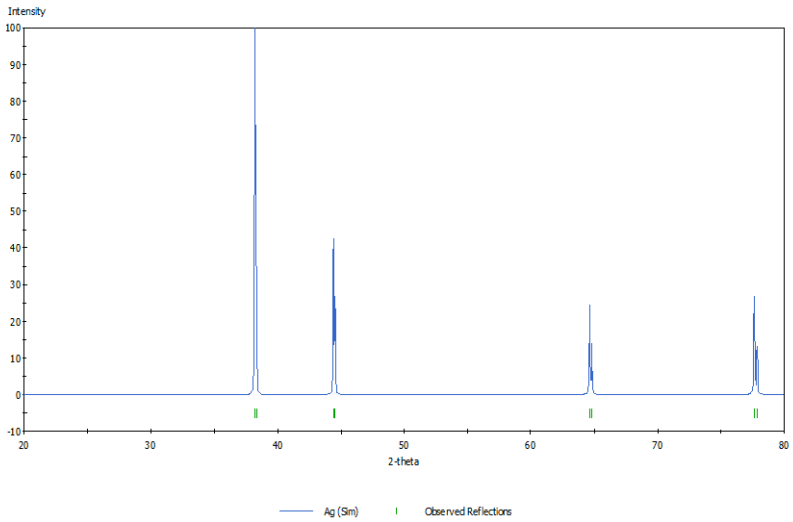

Figure 4.14 Simulated XRD pattern of Ag Face Centered structure

X-ray diffraction of the Ag nanoparticles prepared by precipitation method reveals that they are polycrystalline in nature with the prominent peak 111 of Ag. It exhibits FCC structure. The results are very close to the JCPDS data (893722) with lattice parameter 4.085 Å (a) and space group 225. The optimized FCC lattice parameter is 4.085 Å which is very close to the experimental value 4.0755 Å.

Table 4.2 Miller indices of Ag structure

h	k	l	2Θ (SIMULATED)	INTENSITY (%)
1	1	1	38.2	100
2	0	0	44.4	42.9
2	2	0	64.65	24.25
3	1	1	77.65	26.77

The self-consistent method of convergence of the structure is used to optimize the lattice parameter. The X-ray diffraction is simulated and the XRD results are similar to that of the experimental XRD spectrum with slight deviation in the order of 0.05 to 0.06%. The band gap energy of Ag shows that there is a merging of valence band and conduction band.

4.4.2.2 *ab initio* STUDIES OF ELECTRONIC PROPERTIES of Ag

The calculations of electronic characteristics; total electronic energy E, band energy dispersion E (k) and density of states of Ag structure are simulated using the CASTEP code. Figures 4.15 and 4.16 illustrate the band structure and density of states of Ag respectively.

The total energy per atom convergence tolerance, smearing width and Fermi energy convergence tolerance are taken as $2x10^{-6}$ eV, 3×10^{-7} eV, 0.1 eV and 3×10^{-8} eV respectively. The band structure and density of states of Ag are calculated using LDA and are shown below;

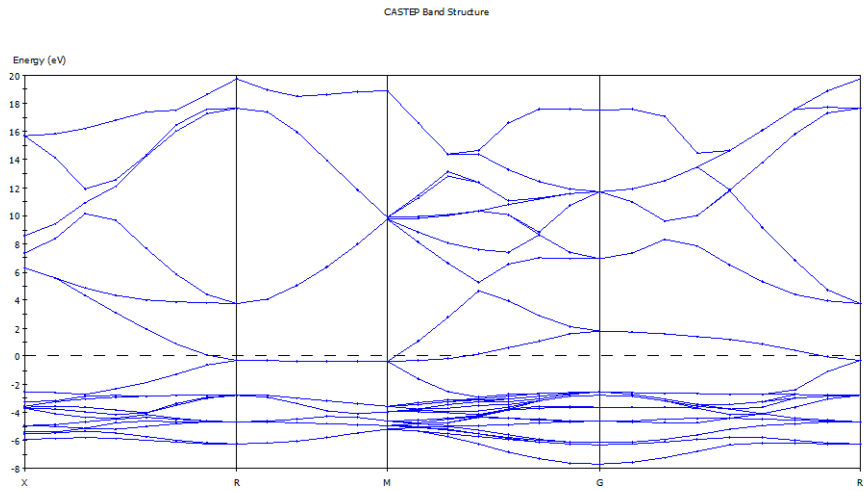

Figure 4.15 Band Structure of Ag

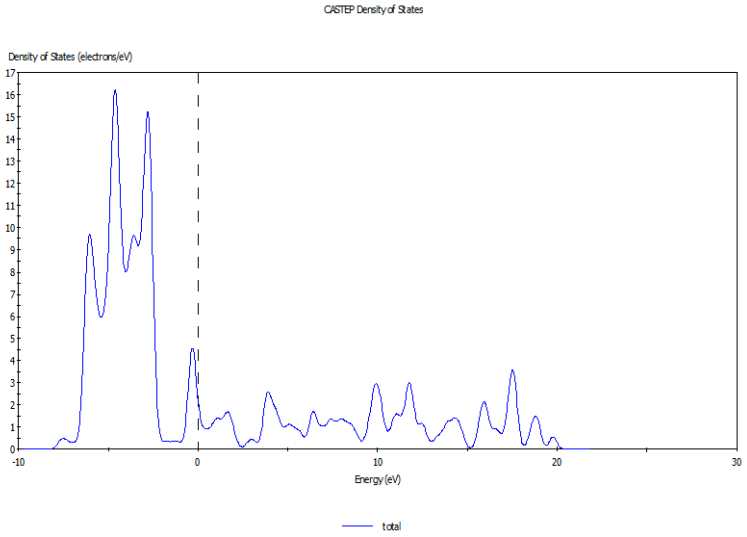

Figure 4.16 Density of states of Ag (LDA)

4.4.2.3 *ab initio* Studies of Optical Properties of Ag

Absorption, reflectivity, refractive index and extinction coefficients have been measured for Ag (FCC). The simulated absorption, reflectivity, refractive index and extinction coefficient studies of silver (Ag) are given in Figures 4.17, 4.18 and 4.19 respectively. Also the optical response functions for the Ag are calculated with the LDA and compared to the experimental data.

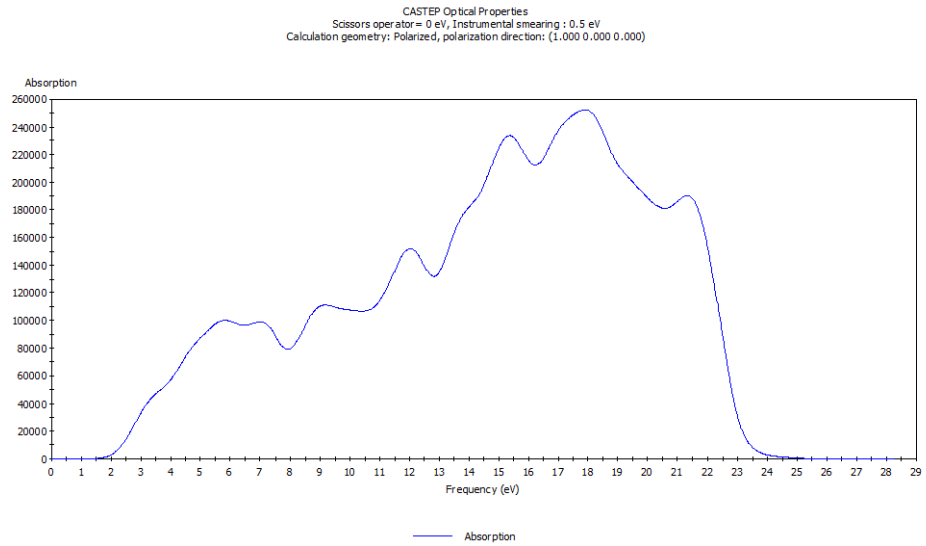

Figure 4.17 Absorption Spectrum of Ag (LDA)

It has been observed that the maximum absorption is at 17.5eV. The absorption study of the material is very important. Silver nanoparticles should have sufficient energy to penetrate into the cell walls of the bacteria or the biological cell structure of the animal or human.The maximum absorption energy of Ag is found as 17.5 eV which is higher than that of Iron. Hence it is sufficient to penetrate into the biological cells and react with enzymes and DNA structure effectively than that of Fe. More the absorption energy more will be the permeability of the nano material into the biological cells. It is evidently observed in the antibacterial study of iron and silver nanoparticles.

The reflectivity with wavelength was simulated using LDA is shown below. In order to verify the counterpart of absorption and transmittance, the reflectivity of Ag has been studied. It has been observed that the reflectivity is maximum 22.5 eV

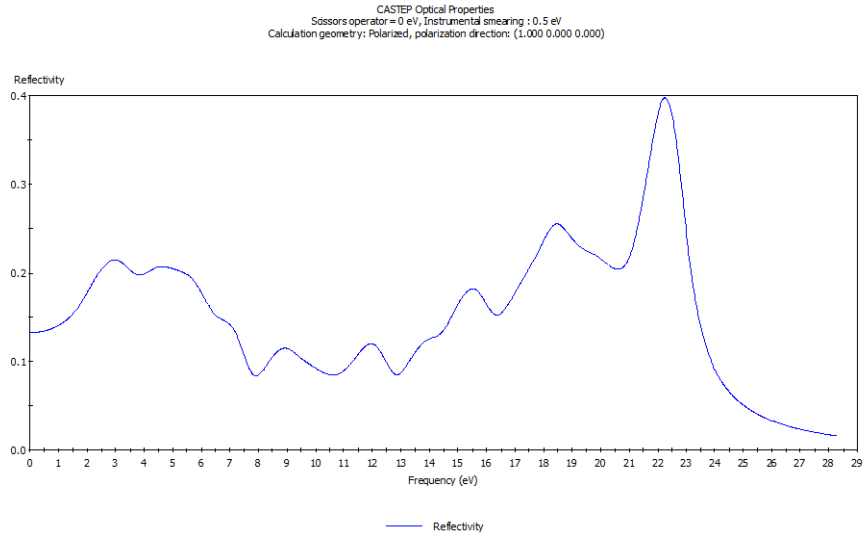

Figure 4.18 Reflectivity of Ag (LDA)

The refractive index of the Ag with different wavelength was calculated and is shown below,

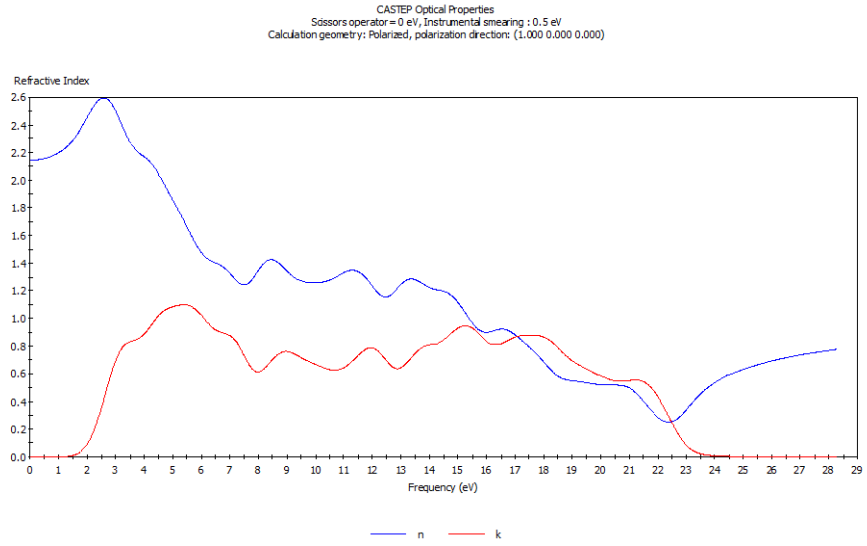

Figure 4.19 Refractive index and Extinction Coefficient of Ag (LDA)

The refractive indices (n) and extinction coefficient (k) are fluctuating in the higher range from 7 to 20 eV and decrease gradually.

4.4.2.4 *ab initio* Studies of Dielectrical Properties of Ag

The calculations of dielectric function, conductivity and loss function of Ag structure were simulated using the CASTEP code. Figures 4.20, 4.21 and 4.22 illustrate the dielectric function, conductivity and loss function of Ag respectively.

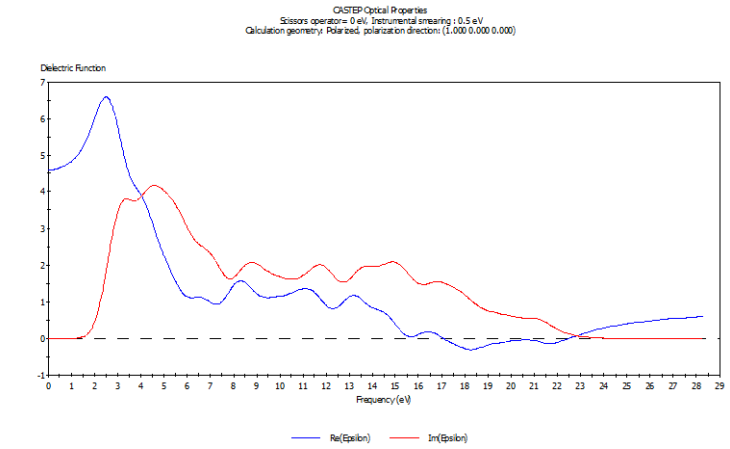

Figure 4.20 Dielectric Function of Ag (LDA)

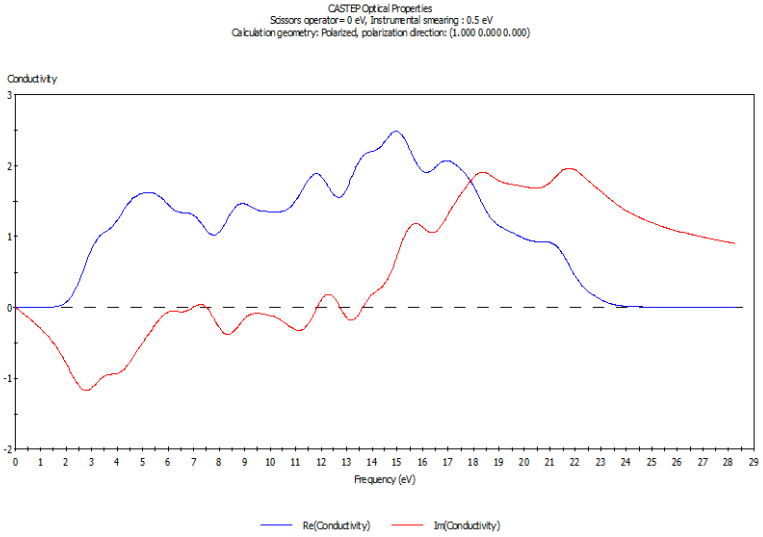

Figure 4.21 Conductivity of Ag (LDA)

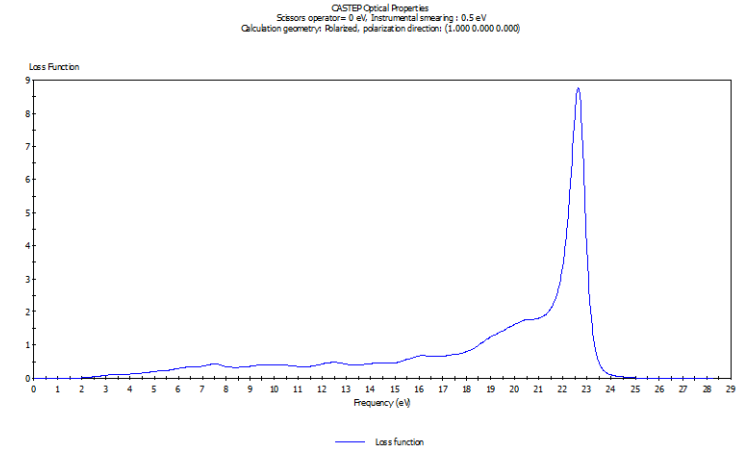

Figure 4.22 Loss Function of Ag (LDA)

The dielectric behavior of the material is necessary to know the interaction of the material with the medium or environment in which the material is present.

In the present study the nanoparticles of silver are subjected to have interaction with the bacteria, enzymes and body cells of rabbits. An attempt is made to study the dielectric behavior of silver nanoparticles in bacteria and enzymes medium and find factors causing the biological changes in the cell structure.

4.5 CONCLUSION

Using the first-principle calculations the electronic structures and band parameters for Fe and Ag were obtained within the Local Density Approximations. It is found that the structure, band gap, energy levels, band dispersion and optical properties calculated by LDA are comparable with the experimental results. The expected energy of Iron nanoparticles to penetrate into the walls of the bacteria or any biological system can be estimated using this technique. It is observed that the more absorption energy, the more will be permeability of the nano-material into the biological cells.

In the present study the nanoparticles of Iron are subjected to have interaction with the blood medium, bacteria and enzymes. An attempt is made to study the dielectric behavior of iron nanoparticles in blood and enzymes medium and find factors causing biological changes in the cell structure.The dielectric behavior of the material is necessary to know the interaction of the material with the medium or environment in which the material is present.Similar to Fe, the theoreitical calculations of Ag are found in good agreerment with the experimental results. Silver nanoparticle should have sufficient energy to penetrate into the cell walls of the bacteria or the biological cell structure of the animal or human.The maximum absorption energy of Ag is found as 17.5 eV which is higher than that of Iron. Hence it is sufficient to penetrate into the biological cells and react with enzymes and DNA structure effectively than that of Fe.

In the present study the nanoparticles of silver are subjected to have interaction with the bacteria, enzymes and body cells of rabbits. An attempt is to be made to study the dielectric behavior of silver nanoparticles in bacteria and enzymes medium and find factors causing the biological changes in the cell structure.The above attempts made in theoritical studies of Fe and Ag will lead a new opening to the forthcoming researchers. Further, the theoritical study could be extended to probe the interactions between nanoparticles and biological systems to have a prior understanding on the *in-vivo* or *in-vitro* studies.